Signal-to-noise ratio evaluation of fibre Bragg gratings for dynamic strain sensing at elevated temperatures in a liquid metal environment.

Ben De Pauw, Alfredo Lamberti, Ali Rezayat, Julien Ertveldt, Steve Vanlanduit, Katrien Van Tichelen, Thomas Geernaert, and Francis Berghmans,

***Abstract*—Vibration measurements of the fuel assembly of a nuclear reactor are a very useful tool to determine the health and lifetime of the reactor core. The importance of these measurements is exacerbated in the new generation of heavy liquid metal reactors, where the fuel assembly is exposed to a corrosive molten metal coolant at 300°C and where the space between the individual fuel pins is limited to a few millimeters. In this paper we consider fibre Bragg gratings as potential candidates for carrying out fuel pin vibration measurements in such an environment. We describe a dedicated method to integrate fibre Bragg gratings in a fuel pin and we subject this pin to conditions close to those encountered in a real heavy liquid metal reactor. More specifically, we report on the performance of draw tower gratings used as a vibration sensor when the fuel pins are immersed in heavy liquid metal at 300°C for up to 700 hours. The performance evaluation is based on monitoring the signal-to-noise ratio of the grating's spectral response as a function of time. We show that accurate detection of the Bragg peak becomes very challenging after 400 hours of exposure. Additionally, we succeed to extend the useful lifetime with a factor of two by using an appropriate integration of the fiber in the fuel pin and by using an alternate peak detection algorithm.**

***Index Terms*—optical fiber measurements, nuclear power generation safety, vibration measurement**

I. Introduction

DYNAMIC strain measurements can provide information that is valuable to derive the health of a structure [1], [2], [3], [4]. In this study, the structure that is considered is the fuel assembly in a heavy liquid metal (HLM) nuclear reactor core. This assembly consists of a collection of fuel pins that is subjected to the flow of the liquid metal reactor coolant. The design of the fuel pins reported here is that of the nuclear research reactor MYRRHA[5] that will be built at the Belgian Nuclear Research Centre (SCK•CEN). The coolant is molten lead-bismuth eutectic (LBE, melting point 123.5°C) at temperatures up to 300°C. Information derived from dynamic strain measurements inside this fuel assembly is required to understand the interaction between the flow of the coolant and the fuel assembly. From this interaction, the fuel assembly lifetime can be estimated and the mechanical design optimized. Since the space between the individual fuel pins of the assembly is limited (only a few millimeters), fibre optic sensors are one of the very few options for measuring the fuel pin vibrations. Such sensors have already been used many times to carry out dynamic strain measurements[2], [6]. Fibre Bragg gratings (FBGs), more specifically, have a proven potential when it comes to measuring vibrations[7], [8], [9], [10].

To perform vibration measurements with FBGs it is necessary to attach the grating to the surface of the component or to integrate it within the component and to ensure adequate strain transfer between component and grating. In this paper we therefore first demonstrate a dedicated method to integrate FBGs in a nuclear fuel pin. We then describe how we exposed the pin to conditions close to those encountered in MYRRHA, as illustrated in Figure 1. Note that the effects of nuclear radiation on the sensors do not need to be taken into account in this study. FBGs will not be used during the actual exploitation of the reactor. They serve as instruments to measure vibrations in a mock-up situation, with the eventual intention to support the optimization of the design of the fuel assembly. Actual (radioactive) fuel pins may nevertheless generate a heat flow, which could influence the pin vibration but this is considered to be a secondary effect. We report on the performance of the FBGs as a strain sensors when the fuel pin is immersed in LBE during thermal cycles. The performance analysis is based on recording the evolution of the signal-to-noise ratio (SNR) of the individual sensors over time. This provides an estimate of the useful lifetime of the sensors in reactor conditions. We show how we can improve the service life of the optical fibre sensors, first by identifying and reducing noise sources (such as non-uniform strain) and second by implementing a Bragg peak detection method that is immune to noise.

II. Experimental setup & sensor integration

In order to perform dynamic strain measurements on the surface of the individual fuel pins within the fuel assembly, the fibre optic sensors need to be adequately attached to their surface. The first step is therefore to define an appropriate procedure to integrate the sensors within the fuel assembly. The design is illustrated in Figure 2. The optical fibre is inserted within a small groove that has been etched on the fuel pin surface. The fibre is then coiled around and attached to the fuel pin surface with an adhesive. We opted to use type I draw tower gratings (DTGs)[11], [12], [13] which are known to feature excellent strength and fatigue characteristics. Although other types of gratings could be considered,

B. De Pauw is with the Brussels Photonics Team B-Phot and the Department of Mechanical Engineering, Vrije Universiteit Brussel, Brussels, Belgium, e-mail: bdepauw@vub.ac.be

author information: B. De Pauw - Vrije Universiteit Brussel (VUB), Brussels Photonics Team (B-Phot), Brussels, Belgium
mail: bdepauw@vub.ac.be - paper citation information: DOI 10.1109/JLT.2014.2377371, Journal of Lightwave Technology

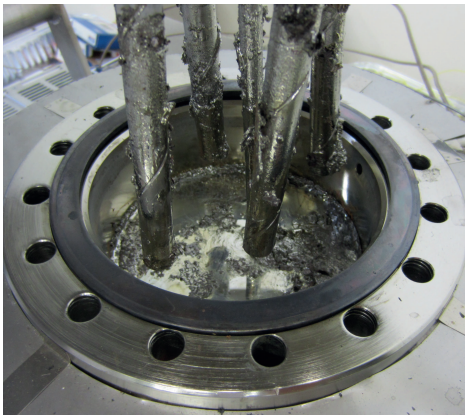

Figure 1: Illustration of the instrumented fuel pins after being immersed in molten lead bismuth eutectic at 300° C

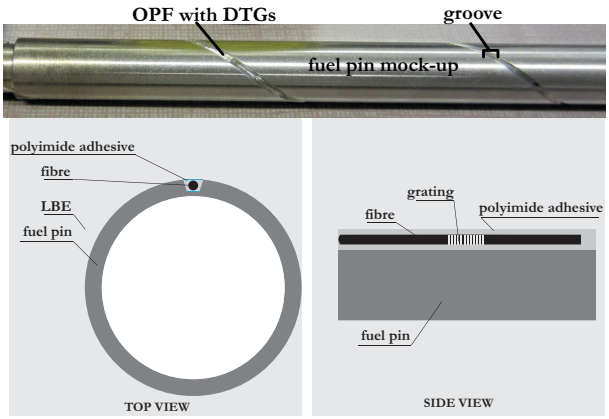

Figure 2: Photograph and scheme of an optical fibre with draw tower gratings embedded in a small helicoidal groove near the surface of the pin.

the former property is especially important during thermal cycles (and shocks) where wavelength shifts up to 10 nm have been encountered. The higher yield strength of DTGs is also particularly important during installation of the fuel pins in the complex reactor vessel structure: as they feature a higher strength than recoated FBGs they are less likely to fail during installation and use. The fibres with DTGs have an ORMOCER (organic modified ceramics)[11], [14], [15], [16] coating. Alternatives have been considered such as metal coated fibres (e.g. aluminium or copper coated fibres from IVG fiber [17]). However, due to the properties of LBE at elevated temperatures, metals should be chosen carefully in order avoid so called liquid metal induced embrittlement. This process causes materials to become brittle as a consequence of exposure to liquid metal at elevated temperatures. Due to the nature of the experimental setup, a portion of the fibre will always be unprotected and exposed to the LBE. Hence metal coated fibres are not adequate. Ceramics on the other hand have shown to be inert to LBE.

The adhesive used for attaching the fibre to the fuel pin is a single component modified polyimide adhesive (Polytec TC P-490)[18], which is rated for continuous operation above 300°C. Upon temperature curing it sets to provide stiff adhesion (shore hardness of D75) between the optical fibre and the fuel pin structure. The substance has adequate out-gassing properties and can serve as a non-abrasive filler while retaining excellent chemical and moisture resistance. The adherence of this adhesive to both glass and stainless steel is excellent. Note that after curing of the adhesive the instrumented fuel pin was kept at 275°C for several hours in order to (further) anneal the gratings.

A. Adhesive particle size analysis

We chose for an adhesive with a small particle size of less than 20 μm. This not only ensures a non-porous protection but also minimally affects the spectral shape of the grating reflection. To verify this we analyzed the effect of the particle size on the local strain relief on the fibre Bragg sensor using a finite element (FE) software package (COMSOL multiphysics)[19]. The strain profile for each particle size was calculated at the fibre edge using a Hertz model (see also [20], [21], [22]) with continuous boundary conditions. We first calculated the stress in the optical fibre perpendicular to the contact plane to validate the finite element model with the Hertz model. The relative Von Mises stresses for a single particle acting on the optical fibre according to the Hertz model and the FE simulations are shown in Figure 3.

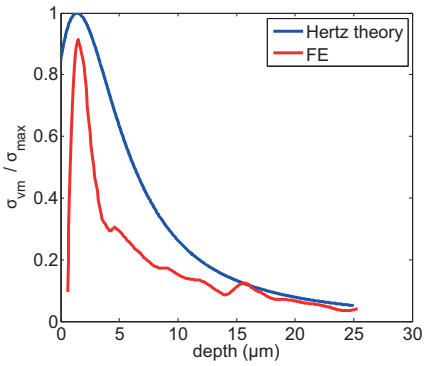

Figure 3: The relative Von Mises stress in the optical fibre perpendicular to the fibre axis) are compared with the Hertz model to validate the finite element (FE) model.

We then determined the grating spectral response using the transfer matrix method[23] for the simulated strain profile of an array of particles. This process was repeated for each particle size. Finally, we compared the obtained spectral response with that of an undisturbed grating by calculating the (Pearson's) correlation coefficient and relative reflectivity. Figure 4 depicts the influence of the adhesive particle size on the distortion of the spectral response of the Bragg sensors. The colored lines in Figure 4 represent the filtered data giving the trend for each particle size. Particle sizes between $100 - 150$ μm yield a non-uniform strain profile at the particle boundaries, that will cause a significant distortion in the spectrum. For the particle sizes of the adhesive used in this paper (i.e. < 20 μm) however, the strain profile will be more uniform and therefore have a less significant effect on the spectrum. The remaining distortion (indicated with the shaded

author information: B. De Pauw - Vrije Universiteit Brussel (VUB), Brussels Photonics Team (B-Phot), Brussels, Belgium
mail: bdepauw@vub.ac.be - paper citation information: DOI 10.1109/JLT.2014.2377371, Journal of Lightwave Technology

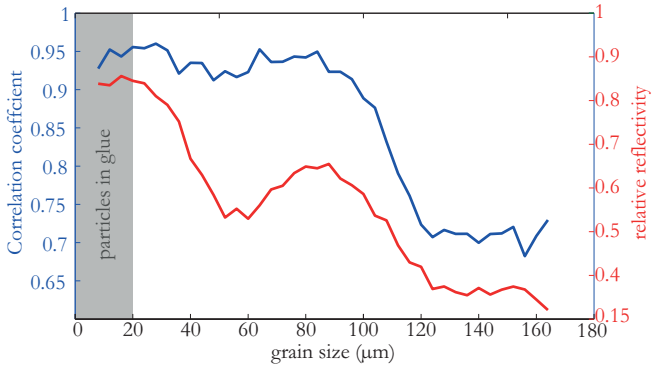

Figure 4: The grain size of an adhesive used to attach an optical fibre to a structure influences the distortion of the fibre Bragg grating response spectrum after curing. The particle sizes of the used adhesive ($< 20\ \mu m$ (gray area)) yield a reduction in reflectivity on the order of 10%.

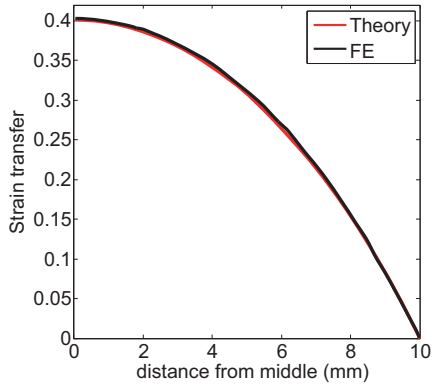

Figure 5: Strain transfer coefficient along the fibre obtained with the FE model and the theoretical model of [24].

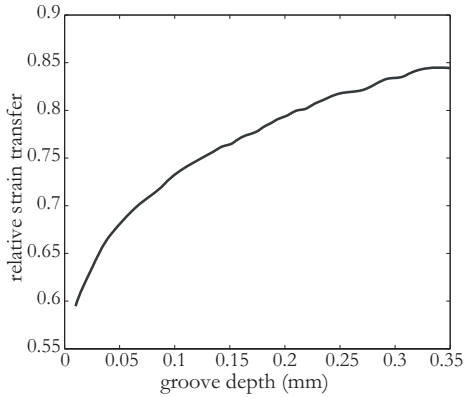

Figure 6: Strain transfer coefficient from fuel pin to fibre as a function of the groove depth

area in Figure 4) leads to a reduction in reflectivity on the order of 10% .

B. Groove depth analysis

As already explained the optical fibre was inserted in a groove that was etched at the fuel pin surface. Since the location of maximal strain is at the surface of the fuel pin, the depth of the groove should be as shallow as possible. On the other hand, a deeper groove provides a larger contact surface area between adhesive and fuel pin. We used COMSOL multiphysics[19] to find the optimal groove depth. First, a part of the fuel pin with a semi-circular groove (diameter = 300 μm) etched at the surface was defined. Silica fibre with a cladding diameter of 125 μm and a coating diameter of 200 μm was placed at the centre of the groove. The remaining gap was filled with the polyimide adhesive. The interfaces were modelled as continuous boundaries. We then applied an axial stress to the fuel pin part only. We define the strain transfer coefficient as the ratio of the resulting strain level in the grating to the strain level at the surface of the fuel pin in absence of the fibre and etched groove. In order to validate this numerical model, we compared it with a theoretical model defined in [24]. A direct comparison between this theoretical model and the used finite element model becomes possible when the groove depth was further increased for the fibre to be completely embedded. The strain transfer distribution along the optical fibre obtained with the FE model and the theoretical model by [24] are plotted in Figure 5. The good agreement between the two models validates the FE approach.

Figure 6 shows the strain transfer simulation results for several groove depths between 0 μm (no groove) and 300 μm (complete immersion of the fibre). The optimal groove depth of approximately 300 μm appears to be a bit larger than the radius of the coated optical fibre. For this groove depth, the resulting strain transfer is maximal and equal to 84%. Further optimization is possible if wider grooves are considered since the thickness of the adhesive layer plays an important role in the transfer of the strain. In this application however, larger grooves should be avoided since these are technically difficult to produce without damaging the cladding of the fuel pin, as can be seen from the wall thickness of only 0.5 mm in Figure 2.

III. Experimental results

In this section we first explain the results of the SNR evaluation of the fibre Bragg sensor response when exposed to the reactor environment. The useful sensor lifetime will prove to be limited if no specific care is taken. Therefore, in the second paragraph of this section we suggest two approaches to improve the useful lifetime.

A. SNR evaluation in reactor environment

The characteristics and the sensing capabilities of the DTG sensors are affected during exposure to high temperatures. For the grating, both the modulation and the mean value of the refractive index decay with time. The decay results in a loss of reflectivity (grating bleaching) and a shift in Bragg wavelength (drift)[25]. The decay rate is a function of the temperature. For long term and high temperature applications, a sufficiently high reflectivity and a stable wavelength shift should be guaranteed. In this study we investigate this effect for the DTGs attached to the surface of fuel pins and subjected

to conditions close to those expected in the MYRRHA reactor. We have exposed DTGs (annealed following the adhesive curing as mentioned earlier) to LBE at 300°C. Several fuel pin models were instrumented according to the integration method described in Section II. After instrumentation, little to no distortion of the spectral response of the Bragg gratings was observed. This also supports the merit of the described integration scheme. These instrumented fuel pin models were then taken from room temperature to molten LBE at 150°C (see also Figure 1). Afterward the temperature was gradually increased with 2°C per minute up to the nominal reactor core temperature of 300°C. This temperature was adjusted with a PID controller and kept constant during the remainder of the experiment.

We logged the reflection spectra of the DTGs every 5 seconds with a spectral resolution of 5 pm (using a Micron Optics SM125 interrogator)[26]. From these reflection spectra we evaluated the signal-to-noise ratio (SNR) of each grating response over time without any additional excitation. The SNR is defined as the ratio between the maximum reflected power and the noise floor (at wavelengths in the vicinity of the Bragg peak). Figure 7 shows the SNR of a selected DTG as a function of time. The experimental data is represented with dots. As expected, the SNR exhibits a gradual decrease over time[25], [27], [28], [29], [30]. The thermal decay of the index modulation related to this process can usually be described with an exponential decay (first order Arrhenius) function. The fitted function is given by:

$$\begin{aligned} &\text{SNR} = a \cdot e^{b \cdot t} \\ &\text{with } a = 8.3 \pm 0.18 \text{ , } b = -1.6 \pm 0.75 \cdot 10^{-3} \end{aligned} \tag{1}$$

and is represented in Figure 7 as a solid line. During the first few hours, the fit underestimates the experimental data. This underestimation can be explained first by the transient nature of the temperature shock upon immersion and then by the gradual increase in temperature. At this stage, the materials exposed to the LBE environment are still settling, i.e. residual strain is removed. After 600 hours we again notice a discrepancy between the fitted data and the experimental results. This can be the result of DTGs annealing or degradation of the adhesive or coating.

Figure 7 also shows the effect of the decay in index modulation on the spectral response of the selected grating at different moments in time. The decrease in Bragg peak amplitude is clearly visible up to 200 hours of exposure. Beyond that time, non-uniform stresses in the adhesive layer are formed, which lead to non-uniform strain distributions over the length of the grating and thus to distortion of the Bragg response. During exposure to the corrosive and high temperature environment simulating the nuclear reactor core, small cracks can occur in the bond layer. These cracks will be filled quickly with the highly fluid LBE coolant releasing the stresses in the bond layer locally. Cracks occur in random places and an increasing number of cracks are created over time. The amount of distortion of the spectrum therefore increases over time. The combined effect of these phenomena would make dynamic strain measurements increasingly difficult.

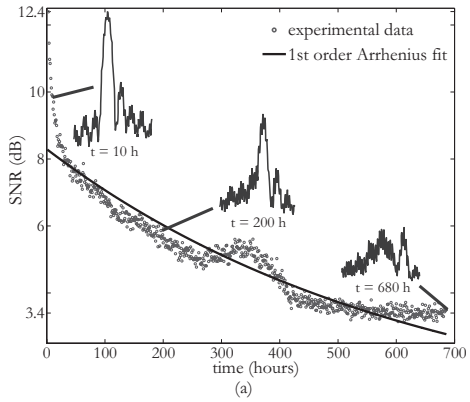

Figure 7: SNR of the spectral response of DTGs in the reactor environment as a function of time. The shape of the spectra at different times is shown for sake of illustration.

To evaluate the exposure time as of which reliable dynamic measurements would no longer be possible, we relied on the measured static spectral response. Controlled dynamic excitation of the fuel pins inside the reactor environment is very challenging and hence we used the frequently logged spectral responses to estimate the dynamic measurement capability of the gratings for different SNRs. Every hour a subset of 100 consecutive spectra was used to generate a simulated vibration output. First a sine wave input was defined with a 5 pm wavelength shift amplitude. This wavelength shift corresponds to strain values that we believe is representative for the actual fuel pins. For each step of this sine wave, a random spectrum of the subset was selected and shifted accordingly. Comparing the input wave with the estimated Bragg wavelength shift in every step yields an estimation of the performance of the DTGs for vibration measurements at that moment in time. The result is shown in Figure 11(a). The comparison is given by the coefficient of determination or R^2 value. The Bragg peak was identified using a traditional Gaussian fitting algorithm[31]. Figure 11(a) indicates that in the first 400 hours of exposure - when the SNR is still high - the R^2 value is larger than 90%. However, around 400 hours of exposure to the LBE environment at 300°C, the spectral response of the gratings has degraded significantly, resulting in a R^2 value below 10%. To identify the acceptable SNR range, we evaluate the SNR as a function of the R^2 value (Figure 8). We then fitted an exponential decay to the resulting curve and determined the 1/e point (represented with the solid vertical line in Figure 8). At this point the SNR is still 4.6 dB but peak distortion makes it more difficult to identify a unique Bragg wavelength as the SNR decreases further. As a consequence, vibration measurements with the current parameters for a grating become prone to errors. In conclusion, the spectral distortion rather than the thermal decay of the reflectivity is the bottleneck when using DTGs for dynamic strain sensing in molten LBE at elevated temperature. This also means that high temperature gratings or gratings with a higher initial reflectivity than DTGs would not necessarily lead to better results. Once spectral broadening can be reduced,

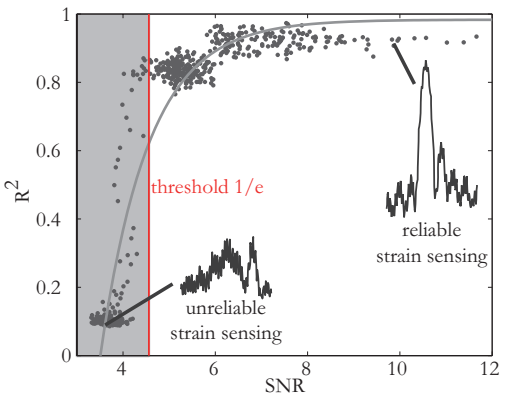

Figure 8: R^2 value as a function of SNR. The 1/e point (red) indicates the critical point where dynamic measurements become unreliable.

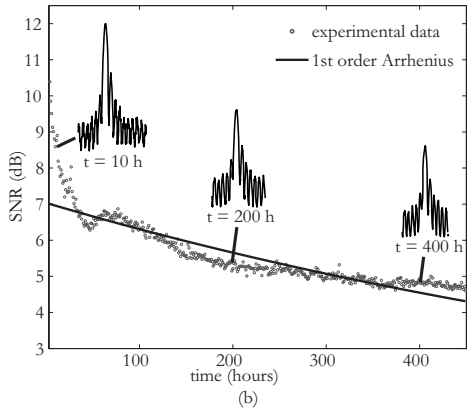

Figure 9: SNR of the spectral response of draw tower gratings in the reactor environment as a function of time for the design *with* glass capillary.

these other types of gratings will allow further increasing the lifetime of the sensors. In the following subsection we explore two approaches to tackle the issue of spectral distortion.

B. Improvement of sensor useful time

To improve the useful lifetime of the sensor we first dealt with the origin of the spectral distortion. In Section II we have shown that the size of the grain of the adhesive bonding influences the distortion of the spectrum. Moreover, we explained that cracks in the bond layer also lead to distortion of the spectrum. As a result dynamic strain measurements become increasingly difficult. To accommodate for this we altered the integration design to avoid direct contact of the grating with the polyimide adhesive.

At the exact location of the FBGs the fibre was protected with a small glass capillary. This capillary ensures uniform strain transfer from the structure to the gratings while sacrificing a couple of millimeters of localized sensing. The inner diameter of the capillary was 300 μm and the wall thickness 200 μm. To accommodate for the size of the capillary, we increased the size of the groove slightly. As a result there was no direct contact between the adhesive and the grating. By consequence the grain size and groove depth have a less significant effect on the spectral response of the grating. Several fuel pin models were instrumented and taken from room temperature to molten LBE at 150°C. Again the temperature was gradually increased (2°C/min) up to 300°C and kept constant afterward. For this new design the SNR could be evaluated from the spectral response. This is shown in Figure 9. In this design the first order Arrhenius fit yields

$$\begin{aligned} &\text{SNR} = a \cdot e^{b \cdot t} \\ &\text{with } a = 7.0 \pm 0.07 \text{ , } b = -1.1 \pm 0.04 \cdot 10^{-3}. \end{aligned} \tag{2}$$

The effect of spectral distortion on the SNR values become clear when comparing the exponential decrease of the SNR values without (Figure 7) in the first case and with (Figure 9) the glass capillary around the grating. Spectral distortion leads to a faster decrease in SNR and thus decrease the serviceability time of the FBGs. When the glass capillary is added, the decay of the SNR can be attributed to the loss in reflectivity alone. The shape of the Bragg spectrum is now retained since only a uniform strain field acts on the fibre sensor. There is no more ambiguity in the position of the Bragg peak and thus the R^2 value for simulated dynamic measurements (sine with 5 pm amplitude) remains high (see Figure 11(b)). This leads to the conclusion that adding the glass capillary in the integration design improves the sensor useful time beyond the previously identified limit of 400 hours.

The second approach to deal with the decreasing SNR consists in using a more advanced Bragg wavelength identification technique. Sensing with FBGs usually relies on the accurate detection and/or estimation of the Bragg wavelength. To identify this peak in a spectrum several algorithms can be adopted[32], [33]. We therefore compared several common and less common algorithms to try to improve the useful sensor time. Figure 10 compares a maximum detection, a quadratic and cubic interpolation, a Gaussian fit[31], a centroid approximation and a phase[34], [35] and cross correlation[36] technique. The horizontal axis is the time given in hours while the vertical axis gives the Bragg wavelength in arbitrary units. To increase the legibility of Figure 10 and to ease the comparison between the different algorithms, the result for each algorithm has been shifted vertically by 100 pm. From Figure 10, it is clear that from times just over 400 hours of exposure, the quadratic, cubic, maximum interpolation and Gaussian fit algorithm fail. This is the same point in time that was identified in the previous section III-A. The Bragg peak then appears to consist of a number of peaks that are closely spaced and that have equal amplitudes yielding the inaccurate estimation of the peak. In contrast, a cross or phase correlation technique or a centroid approximation seems to be less susceptible to the ambiguity since they do not make any assumption about the shape of the Bragg peak.

On the right-hand side of Figure 10 we quantify the precision of each technique (assuming no other strain or heat sources are present) by calculating the standard deviation of each technique with the (linearized) experimental data. For the quadratic, cubic, maximum and Gaussian technique this

author information: B. De Pauw - Vrije Universiteit Brussel (VUB), Brussels Photonics Team (B-Phot), Brussels, Belgium
mail: bdepauw@vub.ac.be - paper citation information: DOI 10.1109/JLT.2014.2377371, Journal of Lightwave Technology

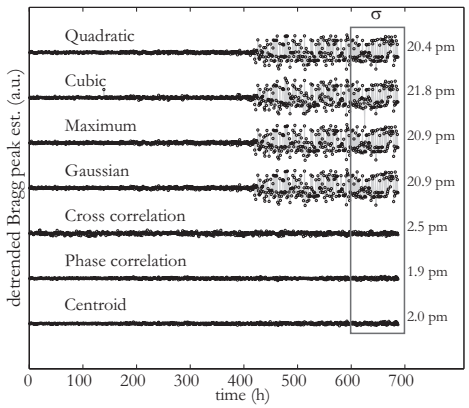

Figure 10: The detrended Bragg peak estimation for several peak detection algorithms. The scatter in the last 100 hours gives an idea about the reliability of the technique at low SNR.

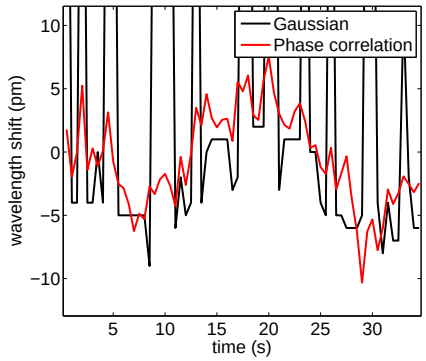

Figure 12: After 700 hours of exposure, a small and slow oscillating signal was applied to the fuel pin mockup. Gaussian peak detection together with phase correlation on the resulting spectral response is shown. This result is very similar to the conclusions from Figure 10.

deviation is close to 20 pm. Finally the cross and phase correlation algorithm and the centroid approximation have a standard deviation of the order of 2 pm.

This result indicates that the phase correlation technique and the centroid approximation are the best candidates for improving the sensor lifetime (even with low SNR). Figure 11(c) shows the R^2 value over time for the used phase correlation technique and centroid approximation using the exact same input (sine of 5 pm) and spectral data as in Figure 11(a). The figure shows that the R^2 value remains larger than 85% for the entire 700 hours of exposure. The uncertainty on the R^2 value does significantly increase at the critical point at just over 400 hours, but it remains below 1.5%. In conclusion, the phase correlation technique and centroid approximation allow extending the useful time of the FBGs, even when the SNR is low.

The suitability of the method described in the previous paragraph has been experimentally confirmed by analyzing a slow oscillating vibration signal applied to the fuel pins. After 700 hours of exposure to the LBE environment, the vessel was opened and the fuel pins were manually excited to generate a small and slow oscillating vibration signal. The resulting spectral responses were analyzed with both a Gaussian peak detection algorithm and a phase correlation technique. An excerpt of the corresponding wavelength shifts is illustrated in Figure 12. Both techniques show similar scatter as determined in Figure 10. It is clear that the Gaussian peak detection is unsuitable after 700 hours of exposure while the phase correlation technique is still able to resolve a significant part of the vibration signal.

IV. Conclusion

In this paper we have illustrated a procedure to integrate draw tower gratings at the surface of a nuclear fuel pin to enable dependable dynamic strain measurements. We confirmed the applicability of the used adhesive based on the grain size and identified the optimal groove depth to ensure reliable strain transfer between the fuel pin structure and the fibre. Using the proposed integration scheme, we have validated the sensors in the high temperature (300°C) and molten metal environment (LBE) of the nuclear reactor core (in absence of radiation). For this validation, we evaluated the SNR of the spectral response of the gratings to define the useful lifetime of the sensor. We showed that this time is limited by the spectral distortion because of a non-uniform strain field introduced by the combination of high temperature and the molten LBE. To improve the useful sensor lifetime, we adapted two approaches. The first approach requires adding a glass capillary at the exact location of the grating. The second approach was based on a comparison of peak detection algorithms. The phase correlation or centroid approximation technique proved to be the most promising. Both approaches allowed increasing the useful lifetime of the draw tower gratings above 700 hours. This period of time is believed to be sufficient to enable a measurement campaign that allows analyzing the dynamic properties of the fuel pins in reactor conditions.

Acknowledgment

The authors gratefully acknowledge the support of the Belgian Nuclear Research Centre (SCK•CEN). The authors would also like to acknowledge the funding received from the Flemish Agency for Innovation by Science and Technology (IWT) for the SBO project grant 110070 (eSHM with AM) and from the Research Foundation Flanders for Thomas Geernaerts post-doctoral fellowship 12D6615N. Belgian Science Policy is acknowledged for the Interuniversity Attraction Pole P7/35 Photonics@be: towards smart photonics in 2020. The COST 299 action FIDES and COST TD1001 action OFSESA are acknowledged for providing networking opportunities and a forum that allowed discussing parts of the results described in this publication. The Flemish Hercules Foundation and Vrije Universiteit Brussel's Methusalem foundation are acknowledged as well.

References

[1] A. P. Adewuyi and Z. S. Wu, "Vibration-based structural health monitoring technique using statistical features from strain measurements,"

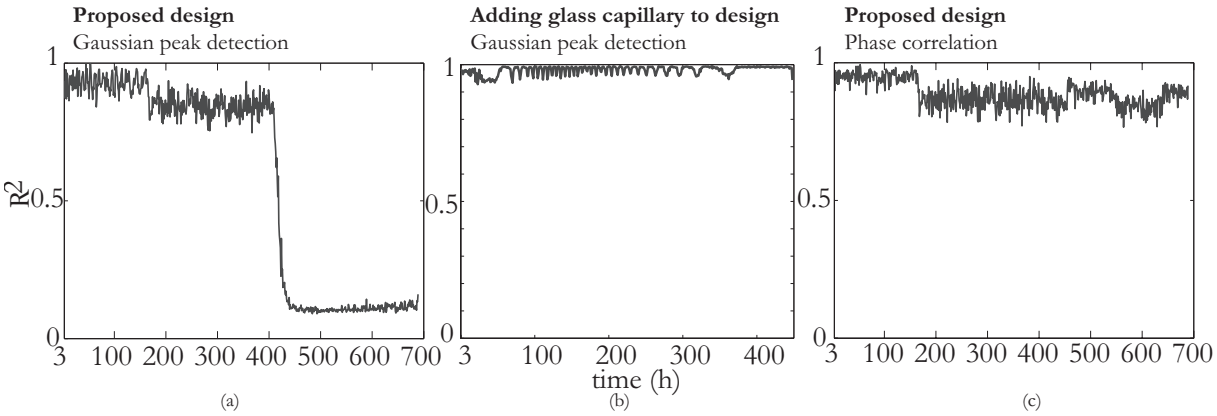

Figure 11: R value as a function of time for the proposed design using traditional techniques (left), the improved design with glass capillary (middle) and original design analyzed with alternate peak detection algorithms (right).

Journal of Engineering and Applied Sciences, vol. 4, no. 3, pp. 38–47, 2009.

[2] W. Ecke, I. Latka, R. Willsch, A. Reutlinger, and R. Graue, "Fibre optic sensor network for spacecraft health monitoring," *Measurement Science and Technology*, vol. 12, pp. 974–980, 2001.

[3] M. Majumder, T. K. Gangopadhyay, A. K. Chakraborty, K. Dasgupta, and D. Bhattacharya, "Fibre Bragg gratings in structural health monitoringPresent status and applications," *Sensors and Actuators A: Physical*, vol. 147, pp. 150–164, Sept. 2008.

[4] G. J. de Villiers, J. Treurnicht, and R. T. Dobson, "In-core high temperature measurement using fiber-Bragg gratings for nuclear reactors," *Applied Thermal Engineering*, vol. 38, pp. 143–150, May 2012.

[5] H. Aït Abderrahim, P. Baeten, D. De Bruyn, and R. Fernandez, "MYRRHA A multi-purpose fast spectrum research reactor," *Energy Conversion and Management*, vol. 63, pp. 4–10, Nov. 2012.

[6] L.-H. Kang, D.-K. Kim, and J.-H. Han, "Estimation of dynamic structural displacements using fiber Bragg grating strain sensors," *Journal of Sound and Vibration*, vol. 305, pp. 534–542, Aug. 2007.

[7] Y. Rodriguez Garcia, J. M. Corres, and J. Giocoechea, "Vibration detection using optical fiber sensors," *Journal of Sensors*, p. 936487, 2010.

[8] M. A. Davis, A. D. Kersey, J. Sirkis, and E. J. Friebele, "Shape and vibration mode sensing using a fiber optic Bragg grating array," *Smart Materials and Structures*, vol. 5, pp. 759–765, Dec. 1996.

[9] B. De Pauw, S. Vanlanduit, K. Van Tichelen, T. Geernaert, K. Chah, and F. Berghmans, "Benchmarking of deformation and vibration measurement techniques for nuclear fuel pins," *Measurement*, vol. 46, pp. 3647–3653, Nov. 2013.

[10] B. D. Pauw, A. Lamberti, S. Vanlanduit, K. V. Tichelen, T. Geernaert, and F. Berghmans, "Signal-to-noise ratio evaluation with draw tower fibre bragg gratings (dtgs) for dynamic strain sensing at elevated temperatures and corrosive environment," *Proc. SPIE*, vol. 9157, no. 91577D-191577D-4, 2014.

[11] "Fbgs technologies, gmbh. www.fbgs.com."

[12] D. Johnson, "Draw-tower process creates high-quality FBG arrays," *Laser Focus World*, no. 10 - Oct, pp. 53–56, 2012.

[13] S. J. Mihailov, "Fiber Bragg grating sensors for harsh environments.," *Sensors (Basel, Switzerland)*, vol. 12, pp. 1898–918, Jan. 2012.

[14] K.-H. Haas and H. Wolter, "Synthesis, properties and applications of inorganicorganic copolymers (ORMOCERs)," *Current Opinion in Solid State and Materials Science*, vol. 4, pp. 571–580, Dec. 1999.

[15] V. Matějec, K. Rose, M. Hayer, M. Pospíšllová, and M. Chomát, "Development of organically modified polysiloxanes for coating optical fibers and their sensitivity to gases and solvents," *Sensors and Actuators B: Chemical*, vol. 39, pp. 438–442, Mar. 1997.

[16] C. G. Askins, M. A. Putman, G. M. Williams, and E. J. Friebele, "Stepped-wavelength optical-fiber Bragg grating arrays fabricated in line on a draw tower," *Optics Letters*, vol. 19, p. 147, Jan. 1994.

[17] IVG-Fiber, "Al1300 and cu1300."

[18] "Polytec gmbh. www.polytec.com/eu," 2011.

[19] Comsol Inc., "www.comsol.com."

[20] K. Johnson, K. Kendall, and A. Roberts, "Surface energy and the contact of elastic solids," *Proc. R. Soc. Lond. A.*, vol. 324, pp. 301–313, 1971.

[21] D. Maugis, "Adhesion of Spheres : The JKR-DMT Transition Using a Dugdale Model," *Journal of Colloid and interface science*, vol. 150, no. 1, pp. 243–269, 1992.

[22] W. Zhang, F. Jin, S. Zhang, and X. Guo, "Adhesive Contact on Randomly Rough Surfaces Based on the Double-Hertz Model," *Journal of Applied Mechanics*, vol. 81, p. 051008, Dec. 2013.

[23] M. A. Muriel and A. Carballar, "Internal field distributions in fiber Bragg gratings," 1997.

[24] R. Wu, B. Zheng, K. Fu, P. He, and Y. Tan, "Study on strain transfer of embedded fiber bragg grating sensors," *Optical Engineering*, vol. 53, no. 8, p. 085105, 2014.

[25] S. Pal, J. Mandal, T. Sun, K. T. V. Grattan, M. Fokine, F. Carlsson, P. Y. Fonjallaz, S. A. Wade, and S. F. Collins, "Characteristics of potential fibre Bragg grating sensor-based devices at elevated temperatures," *MST*, vol. 1131, no. 14, pp. 1131–1136, 2003.

[26] "Micron optics. www.micronoptics.com."

[27] J. Rathje, M. Kristensen, and J. E. Pedersen, "Continuous anneal method for characterizing the thermal stability of ultraviolet Bragg gratings," *Journal of Applied Physics*, vol. 88, no. 2, p. 1050, 2000.

[28] S. Kannan, J. Z. Y. Guo, and P. J. Lemaire, "Thermal stability analysis of UV-induced fiber Bragg gratings," *Journal of Lightwave technology*, vol. 15, pp. 1478–1483, Aug. 1997.

[29] T. Erodgan, V. Mizrahi, P. J. Lemaire, and D. Monroe, "Decay of ultraviolet-induced fiber bragg gratings," *Journal of applied physics*, vol. 76, pp. 73–80, July 1994.

[30] J. Juergens, G. Adamovsky, G. Morscher, B. Park, B. Floyd, A. Corporation, and F. Park, "Thermal Evaluation of Fiber Bragg Gratings at Extreme Temperatures," Tech. Rep. March, NASA/TM, Ohio, 2005.

[31] H.-w. Lee, H.-j. Park, J.-h. Lee, and M. Song, "Accuracy improvement in peak positioning of spectrally distorted fiber Bragg grating sensors by Gaussian curve fitting," *Applied Optics*, vol. 46, no. 12, pp. 2205–2208, 2007.

[32] L. Negri, A. Nied, H. Kalinowsky, and A. Paterno, "Benchmark of Peak Detection Algorithms in Fiber Bragg Grating Interrogation and a New Neural Network for its Performance Improvement," *Sensors*, vol. 11, pp. 3466–3482, 2011.

[33] S. D. Dyer, W. A. Paul, and J. R. Espejo, "Fundamental limits in fiber Bragg grating peak wavelength measurements," *Proceedings of SPIE*, vol. 5855, pp. 88–93, 2005.

[34] A. Lamberti, S. Vanlanduit, B. D. Pauw, and F. Berghmans, "A novel fast phase correlation algorithm for peak wavelength detection of fiber Bragg grating sensors," *Optics Express*, vol. 22, no. 6, pp. 7099–7112, 2014.

[35] A. Lamberti, S. Vanlanduit, B. D. Pauw, and F. Berghmans, "Peak detection in fiber Bragg grating using a fast phase correlation algorithm," in *Proc. SPIE, 9141*, pp. 91410Y–1–91410Y–11, 2014.

[36] C. Huang, W. Jing, K. Liu, Y. Zhang, and G. D. Peng, "Demodulation of Fiber Bragg Grating Sensor Using Cross-Correlation Algorithm," *IEEE Photon. Technol. Lett*, vol. 19, no. 9, pp. 707–709, 2007.